



OPEN

Novel pyridine bearing pentose moiety-based anticancer agents: design, synthesis, radioiodination and bioassessments

Marwa M. Mehany¹, Olfat A. Hammam², Adli A. Selim^{3✉}, Galal H. Sayed⁴ & Kurls E. Anwer⁴

Pyridine compounds are one of the most important heterocyclic derivatives showing wide ranges in biological and pharmacological activities. Green chemistry eliminates or reduces the generation of hazardous compounds. It prevents pollution at a molecular level. The microwave technique used in heterocyclic compound synthesis is also an important branch of green chemistry techniques. In this study, we report designing and synthesizing a new pyridine-bearing pentose moiety via a one-pot multicomponent reaction using D-glucose and also investigate its behavior and reactivity toward some simple and heterocyclic amino derivatives. The chemical structures of the synthesized compounds were characterized and tested for their cytotoxic activities. Some of the test compounds exhibited slight to high cytotoxic activities against Caco2 (colon cancer) cells, HepG2 (hepatocellular carcinoma) cells and MCF-7 (human breast cancer) cells by MTT assay. The results showed clearly that compound 4 and compound 8 displayed strongest to moderate cytotoxic activity against the HepG2, Caco2 and MCF-7 respectively and compound 1 showed good activity against MCF-7 in comparison to the standard anticancer drug doxorubicin. These data were by cytopathological examination. An in-vivo radioactive tracing study of compound 4 proved its targeting ability to sarcoma cells in a tumor-bearing mice model. Our findings suggest that the synthesized compounds may be promising candidates as novel anticancer agents.

Pyridine compounds are one of the most important heterocyclic derivatives widely used in petrochemical industry^{1,2}, catalytic³ and polymer⁴ manufacturing. Heterocyclic chemicals, in particular pyridine, were applied in medicine and biology. The majority of pertinent medicinal compounds have been found to have pyridine scaffolds, offering a huge opportunity for therapeutic intervention⁵. Pyridines act on carbonic anhydrase inhibitors, this vital enzyme found in red blood cells, the mucosa of the stomach, pancreatic cells, and even the renal tubules. It sustains bone resorption, respiration, ureagenesis, gluconeogenesis, electrolyte secretion, and lipogenesis. It also maintains acid–base equilibrium. These processes involve CA isoenzymes, which are significant therapeutic targets that can be blocked to treat a range of illnesses, including cancer^{6,7}. Liu and colleagues (2019) identified 2-amino-4-(1-piperidine) pyridine derivatives as new ALK/ROS1 dual inhibitors resistant to crizotinib⁸. Pyridines act as EGFR and HER-2 kinase inhibitors. EGFR family includes EGFR (HER1/ErbB-1), ErbB-2 (HER2/neu), ErbB-3 (HER3), and ErbB-4 (HER4). One gene linked to breast cancer is human epidermal growth factor receptor 2⁹. Overall pyridines function on a variety of targets, including topoisomerases, phosphoinositide 3-kinase, maternal embryonic leucine zipper kinase, C-met, EGFR, HER-2 kinase, CDK, PIM-1 kinase, and possible cytotoxic compounds⁵. Pyridine derivatives have partially harmful effects on the environment and humans and there are requirements for converting them into safe and useful products^{10,11}. During the last decades, derivatives of pyridine showed a range of biological and pharmacological activities such as antagonist (for anti-inflammatory activity as p38 α /MAPK14 inhibitor), anti-inflammatory, analgesic, herbicidal, anthelmintic, anticancer, antiviral, antioxidant, antimitotic, acaricidal, insecticidal and antimicrobial activities^{12–20}. Furthermore, synthetic heterocyclic compounds containing nitrogen atoms have proven to have significant and diverse therapeutic potential. Thiazole, pyrazole, diazene and pyrimidine derivatives are reported to exhibit promising industry and biology applications^{21–25}. Carbohydrates are natural products that are considered environmentally

¹Laboratory Department, Chemistry Unit, Police Hospital, Agouza, Cairo, Egypt. ²Pathology Department, Theodor Bilharz Research Institute, Giza, Egypt. ³Labeled Compounds Department, Hot Laboratories Centre, Egyptian Atomic Energy Authority (EAEA), Cairo 13759, Egypt. ⁴Heterocyclic Synthesis Lab., Chemistry Department, Faculty of Science, Ain Shams University, Abbassia, Cairo 11566, Egypt. ✉email: adli_a_selim@yahoo.com

sustainable compounds with a broad fascinating activity such as solubility in many polar solvents. This is because of the large number of OH groups that are present in their molecule skeletons. Carbohydrate derivatives showed excellent therapeutic action against diabetes, cancer, HIV infection, etc. Also, their anti-inflammatory, antibiotics, antiviral, antimalarial and the properties of the glycosylation inhibitors. The heterocyclic derivatives from carbohydrates are openly used in our daily lives as detergents, cosmetics, clothes, food, lumber paper, sweetening agents, and so on. Furthermore, chemical transformations that involve using glucose or hexoses together with other industrially and biologically useful chemical compounds have become a top research point in the last decades. This is because glucose and/or hexoses are more superabundant and considered one of the most important natural renewable resources. Carbohydrates and their heterocyclic derivatives have an important place in different chemistry fields and their synthesis depends on microwaves are considered one of the most economical and versatile green techniques for the synthesis of many heterocyclic compounds²¹. Zhang et al. synthesized compounds containing pentose moiety and discovered that these compounds demonstrated a clear inhibitory effect on A450 lung cancer cells²⁶. Green chemistry is the chemical process design science that eliminates or reduces hazardous compounds generation. It prevents pollution at a molecular level. The use of microwave technique in the synthesis of heterocyclic compounds is also an important branch of green chemistry techniques. One-pot multicomponent reaction²² is one of the most important tools for synthesis with facile execution, effectiveness for its productivity and highly diverse products generation in a single running and from easily starting materials. So, such techniques have much more attention because of their safety on the environment, improvement of the yield and time of the reaction and more convenient, and easily synthetic procedures which are highly energy efficient. Compared with microwave irradiation and conventional techniques are more environmentally tolerant, easily controlled, and friendly environmentally. As an advantage, many heterocyclic reactions were carried out in shorter reaction times, higher yields, and milder and cleaner conditions^{27–30}. So now, this green synthesis type is considered a significant technique in heterocyclic chemistry synthesis because of its economy, simplicity, and mild conditions. The ongoing attempts to synthesize novel heterocycle derivatives are motivated by their previously successful uses in industry and biology^{31–42}. In this study, we report designing and synthesizing a new pyridine-bearing pentose moiety via a one-pot multicomponent reaction using D-glucose^{43–45}, and also investigate its behavior and reactivity toward some simple and heterocyclic amino derivatives. Also, the reactions were pressed using the thermal method along with the one-pot microwave technique. Furthermore, a comparison between the percentage yields and consumed times, which resulted from the two techniques was performed. The novel isolated products were illustrated by using different spectroscopic and analytical tools. The pharmacokinetic behavior of the most effective compound was studied with the aid of a radiolabeling technique to evaluate its targeting ability to tumor sites in the tumor-bearing mice model. The used radioisotope is iodine-131 which has a dual emission of both beta particles and gamma photons which makes its ability to be used as a theranostic agent^{46–48}. The primary goal of this study was to design and synthesize new pyridine derivatives bearing pentose moiety for cancer-targeted chemo/radioisotope therapy.

Experimental

Materials and methods

All solvents, reagents and chemicals were bought from Sigma Aldrich. The used solvents were purified according to the standard methods. TLC was carried out on the plates of silica gel (Merck Kiesel gel 60F254, BDH) to monitor the progress of all synthesized compounds homogeneity and reactions. Microwave reactions were carried out with microwave reactor Anton Paar (monowave 300) using 10 mL borosilicate glass vials. All melting points were measured on a digital Stuart electric melting point apparatus “SMP3” and were uncorrected. Infrared spectra measurements (cm^{-1}) were determined using KBr disks on a PerkinElmer 293 spectrophotometer. The $^1\text{H-NMR}$ and $^{13}\text{C-NMR}$ spectra were measured on a Varian Mercury 300 MHz spectrometer. All synthesized compounds were dissolved in DMSO-d_6 as a solvent using tetramethyl silane as an internal standard. A GC-2010 Shimadzu Gas chromatography mass spectrometer (EI, 70 eV) was used for Mass spectrometry measurements. A Perkin-Elmer CHN-2400 analyzer was used for elemental microanalyses (CHN), the data were found to be in good agreement within $\pm 0.4\%$ of the theoretical values. No-carrier-added [^{131}I]NaI was received as a gift from RPF (Radioisotopes-Production-Facility), Egyptian Atomic Energy Authority (EAEA). A NaI (TI) scintillation counter (Scaler Ratemeter SR7 model, the United Kingdom) was used for γ -ray radioactivity measurement.

The reported compounds syntheses

The following sections will be given, the preparation of the starting material ethyl-6-amino-5-cyano-2-methyl-4-(1,2,3,4,5-pentahydroxypentyl)nicotinate (**1**), followed by compound **1** reaction procedures with some amino derivatives.

Ethyl-6-amino-5-cyano-2-methyl-4-((1S,2R,3R,4R)-1,2,3,4,5-pentahydroxypentyl) nicotinate (1)

A mixture of glucose (1.98 g, 10 mmol), malononitrile (0.66 g, 10 mmol), ethyl acetoacetate (1.30 mL, 10 mmol) and ammonium acetate (1.16 g, 15 mmol) in ethanol (10 mL) was refluxed for 2 h. The solid precipitated after cooling was collected by filtration, washed with ethanol/water (1:1) and crystallized from ethanol to form pale yellow crystals **1** (m.p 120–122 °C). IR (cm^{-1}) ν : 3381 (OH), 3323, 3224 (NH_2), 2218 (CN), 1721 (C=O), 1648 (C=N). $^1\text{H-NMR}$ (300 MHz, DMSO-d_6) δ (ppm): 1.19 (t, 3H, $\text{CH}_3\text{CH}_2\text{O}$, $J=6$ Hz), 2.38 (s, 3H, CH_3 -pyridine), 2.50–3.30 (broad, 5H, CH_2 & 3CH-glucose), 4.12 (q, 2H, $\text{CH}_3\text{CH}_2\text{O}$, $J=6.6$ Hz), 4.69 (d, 1H, CH-glucose, $J=3.4$ Hz), 6.00–6.60 (m, 5H, 5OH, D_2O Exchangeable), 8.88 (s, 2H, NH_2 , D_2O exchangeable). $^{13}\text{C-NMR}$ (300 MHz, DMSO-d_6) δ (ppm): 14.1, 20.9, 42.9, 60.9, 63.6, 94.9, 115.3, 115.4, 120.0, 143.6, 143.7, 148.1, 152.8, 159.3 and 169.2. MS (m/z): 355 (M^+ , 31.30%). Anal. Calcd for $\text{C}_{15}\text{H}_{21}\text{N}_3\text{O}_7$ (355): C, 50.70; H, 5.92; N, 11.83. Found: C, 50.67; H, 6.04; N, 11.74.

General procedure for synthesis of compounds (2–12)

A solution of **1** (3.55 g, 10 mmol), one drop of concentrated sulphur acid in DMF (10 mL) was refluxed for 6–24 h with either aniline (0.93 mL, 10 mmol), 4-methoxy aniline (1.23 g, 10 mmol), 3-aminophenol (1.09 mL, 10 mmol), 4-aminoacetophenone (1.35 mL, 10 mmol), sulphaguanidine (2.14 g, 10 mmol), 4-aminoazobenzene (1.97 g, 10 mmol), 5-amino-2,3-dihydrophthalazine-1,4-dione (1.77 g, 10 mmol), 2-aminothiazole (1.00 g, 10 mmol), 4-amino-N-(thiazol-2-yl)benzenesulfonamide (2.55 g, 10 mmol), 4-amino-N-(pyrimidin-2-yl)benzenesulfonamide (2.50 g, 10 mmol), 4-aminoantipyrine (2.05 g, 10 mmol). After cooling, the mixture was poured onto cold ice water, the formed solid was collected by filtration, and recrystallized from proper solvent (supplementary file).

(a) Ethyl-6-amino-5-cyano-2-methyl-4-((1R,2S,3S,4S)-1,2,3,4-tetrahydroxy-5-(phenylamino)pentyl)nicotinate 2.

Yellow crystals from methanol (m.p. 180–182 °C). IR (cm⁻¹) ν : 3382 (OH), 3324, 3225 (NH₂), 3.099 (NH), 2218 (CN), 1721 (C=O), 1648 (C=N). ¹H-NMR (300 MHz, DMSO-d₆) δ (ppm): 1.18 (t, 3H, CH₃CH₂O, *J* = 6.1 Hz), 2.50 (s, 3H, CH₃-pyridine), 2.59 (s, 1H, CHNH-Ar), 3.15–3.36 (broad, 4H, CH₂ & 2CH-glucose), 4.07 (q, 2H, CH₃CH₂O, *J* = 6.6 Hz), 4.83 (d, 1H, CH-glucose, *J* = 3.3 Hz), 5.72–5.95 (m, 4H, 4OH, D₂O Exchangeable), 6.80–7.02 (m, 5H, Ar-H), 7.82 (s, 1H, NH, D₂O Exchangeable), 8.50 (s, 2H, NH₂, D₂O Exchangeable). ¹³C-NMR (300 MHz, DMSO-d₆) δ (ppm): 13.8, 21.5, 55.2, 59.5, 60.3, 60.7, 60.8, 109.5, 111.0, 111.1, 114.9, 120.3, 123.5, 133.5, 138.2, 139.7, 144.8, 149.0, 165.5, and 168.5. MS (m/z): 430 (M⁺, 25.63%). Anal. Calcd for C₂₁H₂₆N₄O₆ (430): C, 58.60; H, 6.05; N, 13.02. Found: C, 58.74; H, 5.91; N, 12.99.

(b) Ethyl-6-amino-5-cyano-2-methyl-4-((1R,2S,3S,4S)-1,2,3,4-tetrahydroxy-5-((4-methoxyphenyl)amino)pentyl)nicotinate 3.

Brown crystals from methanol (m.p. 168–170 °C). IR (cm⁻¹) ν : 3383 (OH), 3330, 3200 (NH₂), 3103 (NH), 2220 (CN), 1722 (C=O), 1640 (C=N). ¹H-NMR (300 MHz, DMSO-d₆) δ (ppm): 1.21 (t, 3H, CH₃CH₂O, *J* = 6 Hz), 2.50 (s, 3H, CH₃-pyridine), 2.58 (s, 1H, CHNH-Ar), 3.21–3.30 (broad, 4H, CH₂ & 2CH-glucose), 3.71 (s, 3H, OCH₃), 4.08 (q, 2H, CH₃CH₂O, *J* = 6.5 Hz), 4.78 (d, 1H, CH-glucose, *J* = 3.4 Hz), 5.72–5.94 (m, 4H, 4OH, D₂O Exchangeable), 6.83–7.35 (m, 4H, Ar-H), 8.33 (s, 1H, NH, D₂O Exchangeable), 8.49 (s, 2H, NH₂, D₂O Exchangeable). ¹³C-NMR (300 MHz, DMSO-d₆) δ (ppm): 14.1, 21.4, 55.1, 59.4, 60.4, 60.6, 60.8, 79.6, 109.5, 111.1, 111.4, 113.9, 115.5, 118.7, 119.9, 144.7, 146.4, 149.0, 152.9, 154.3, and 165.5. MS (m/z): 460 (M⁺, 25.70%). Anal. Calcd for C₂₂H₂₈N₄O₇ (460): C, 57.39; H, 6.09; N, 12.17. Found: C, 57.24; H, 6.19; N, 12.09.

(c) Ethyl-6-amino-5-cyano-2-methyl-4-((1R,2S,3S,4S)-1,2,3,4-tetrahydroxy-5-((3-hydroxyphenyl)amino)pentyl)nicotinate 4.

Beige crystals from acetone (m.p. 178–180 °C). IR (cm⁻¹) ν : 3500–3100 (broad, OH & NH₂), 2222 (CN), 1721 (C=O), 1650 (C=N). ¹H-NMR (300 MHz, DMSO-d₆) δ (ppm): 1.20 (t, 3H, CH₃CH₂O, *J* = 6 Hz), 2.49 (s, 3H, CH₃-pyridine), 2.58 (s, 1H, CHNH-Ar), 3.21–3.32 (broad, 4H, CH₂ & 2CH-glucose), 4.07 (q, 2H, CH₃CH₂O, *J* = 6.6 Hz), 4.62 (d, 1H, CH-glucose, *J* = 3.5 Hz), 5.72–5.96 (m, 4H, 4OH, D₂O Exchangeable), 6.19–7.00 (m, 4H, Ar-H), 7.69 (s, 1H, NH, D₂O Exchangeable), 8.50 (s, 2H, NH₂, D₂O Exchangeable), 10.44 (s, 1H, OH, D₂O Exchangeable). MS (m/z): 446 (M⁺, 27.96%). Anal. Calcd for C₂₁H₂₆N₄O₇ (446): C, 56.50; H, 5.83; N, 12.56. Found: C, 56.61; H, 5.89; N, 12.42.

(d) Ethyl-4-((1R,2S,3S,4S)-5-((4-acetylphenyl)amino)-1,2,3,4-tetrahydroxypentyl)-6-amino-5-cyano-2-methylnicotinate 5.

Yellow crystals from dioxane (m.p. 188–190 °C). IR (cm⁻¹) ν : 3401 (OH), 3337, 3230 (NH₂), 3100 (NH), 2222 (CN), 1721, 1680 (C=O), 1650 (C=N). ¹H-NMR (300 MHz, DMSO-d₆) δ (ppm): 1.19 (t, 3H, CH₃CH₂O, *J* = 6 Hz), 2.51 (s, 6H, CH₃CO & CH₃-pyridine), 2.58 (s, 1H, CHNH-Ar), 3.19–3.44 (broad, 4H, CH₂ & 2CH-glucose), 4.07 (q, 2H, CH₃CH₂O, *J* = 6.6 Hz), 4.70 (d, 1H, CH-glucose, *J* = 3.3 Hz), 5.72–5.96 (s, 4H, 4OH, D₂O Exchangeable), 6.54–7.63 (m, 4H, Ar-H), 8.21 (s, 1H, NH, D₂O Exchangeable), 8.50 (s, 2H, NH₂, D₂O Exchangeable). ¹³C-NMR (300 MHz, DMSO-d₆) δ (ppm): 14.2, 21.5, 31.7, 46.1, 59.5, 60.2, 60.5, 60.8, 79.6, 109.5, 111.0, 111.1, 114.9, 118.3, 119.2, 144.8, 146.4, 149.0, 152.9, 154.3, 165.5 and 168.5. MS (m/z): 472 (M⁺, 41.50%). Anal. Calcd for C₂₃H₂₈N₄O₇ (472): C, 58.47; H, 5.93; N, 11.86. Found: C, 58.50; H, 6.03; N, 11.70.

(e) Ethyl-6-amino-5-cyano-4-((1R,2S,3S,4S)-5-((4-(N-(diaminomethylene)sulfamoyl)phenyl)amino)-1,2,3,4-tetrahydroxypentyl)-2-methylnicotinate 6.

Off white crystals from butanol (m.p. > 300 °C). IR (cm⁻¹) ν : 3483–2500 (broad, OH & NH₂), 2266 (CN), 1750–1550 (broad, C=O & C=N). ¹H-NMR (300 MHz, DMSO-d₆) δ (ppm): 1.19 (t, 3H, CH₃CH₂O, *J* = 6 Hz), 2.38 (s, 3H, CH₃-pyridine), 2.50–3.30 (broad, 5H, CH₂ & 3CH-glucose), 4.12 (q, 2H, CH₃CH₂O, *J* = 6.6 Hz), 4.69 (d, 1H, CH-glucose, *J* = 3.4 Hz), 6.00–6.60 (m, 4H, 4OH, D₂O Exchangeable), 6.72 (s, 4H, 2NH₂, D₂O exchangeable), 7.37–7.69 (m, 4H, Ar-H), 8.30 (s, 1H, NH, D₂O Exchangeable), 8.88 (s, 2H, NH₂, D₂O exchangeable). ¹³C-NMR (300 MHz, DMSO-d₆) δ (ppm): 14.2, 21.3, 55.1, 59.5, 60.6, 60.0, 60.2, 79.5, 109.7, 111.0, 111.4, 114.1, 115.5, 118.7, 119.9, 144.7, 146.4, 149.0, 152.9, 154.3, and 165.5. MS (m/z): 551 (M⁺, 33.73%). Anal. Calcd for C₂₂H₂₉N₇O₈S (551): C, 47.91; H, 5.26; N, 17.79; S, 5.81. Found: C, 48.02; H, 5.15; N, 17.89; S, 5.72.

(f) Ethyl-6-amino-5-cyano-2-methyl-4-((1R,2S,3S,4S)-1,2,3,4-tetrahydroxy-5-((4-((E)-phenyldiazanyl)phenyl)amino)pentyl)nicotinate (7).

Yellow crystals from dioxane (m.p. 176–178 °C). IR (cm⁻¹) ν : 3390 (OH), 3320, 3200 (NH₂), 3080 (NH), 2219 (CN), 1721 (C=O), 1651 (C=N), 1450 (N=N). ¹H-NMR (300 MHz, DMSO-d₆) δ (ppm): 1.21 (t, 3H, CH₃CH₂O, *J* = 6.1 Hz), 2.50 (s, 3H, CH₃-pyridine), 2.57 (s, 1H, CHNH-Ar), 3.14–3.57 (broad, 4H, CH₂ & 2CH-glucose), 4.07 (q, 2H, CH₃CH₂O, *J* = 6.5 Hz), 4.76 (d, 1H, CH-glucose, *J* = 3.4 Hz), 5.72–5.97 (m, 4H, 4OH, D₂O Exchangeable), 6.66–7.89 (m, 9H, Ar-H), 8.20 (s, 1H, NH, D₂O Exchangeable), MS (m/z): 534 (M⁺, 29.28%). Anal. Calcd for C₂₇H₃₀N₆O₆ (534): C, 60.67; H, 5.61; N, 15.73. Found: C, 60.55; H, 5.74; N, 15.71.

(g) Ethyl-6-amino-5-cyano-4-((1R,2S,3S,4S)-5-((1,4-dioxo-1,2,3,4-tetrahydrophthalazin-5-yl)amino)-1,2,3,4-tetrahydroxypentyl)-2-methylnicotinate 8.

Pale green crystals from dioxane (m.p. 200–202 °C). IR (cm⁻¹) ν : 3451, 3420, 3382 (OH), 3324, 3223 (NH₂), 3158, 3122 (NH), 2218 (CN), 1721, 1691, 1651 (C=O), 1600 (C=N). ¹H-NMR (300 MHz, DMSO-d₆) δ (ppm):

1.07 (t, 3H, $\text{CH}_3\text{CH}_2\text{O}$, $J=6$ Hz), 2.50 (s, 3H, CH_3 -pyridine), 2.58 (s, 1H, CHNH -Ar), 3.24–3.45 (broad, 4H, CH_2 & 2CH -glucose), 4.05 (q, 2H, $\text{CH}_3\text{CH}_2\text{O}$, $J=6.7$ Hz), 4.76 (d, 1H, CH -glucose, $J=3.3$ Hz), 5.41 (s, 1H, NH, D_2O Exchangeable), 5.72–5.95 (m, 4H, 4OH, D_2O Exchangeable), 6.87–7.47 (m, 5H, Ar-H & NH_2 , D_2O Exchangeable), 11.16 (broad, 2H, 2NH, D_2O Exchangeable). ^{13}C -NMR (300 MHz, DMSO-d_6) δ (ppm): 14.1, 21.4, 59.4, 60.3, 60.5, 60.7, 79.6, 109.4, 116.3, 118.7, 120.6, 126.5, 127.1, 133.8, 142.8, 144.7, 146.4, 148.9, 150.6, 151.4, 161.3, 156.4, and 168.4. MS (m/z): 514 (M^+ , 42.07%). Anal. Calcd for $\text{C}_{23}\text{H}_{26}\text{N}_6\text{O}_8$ (514): C, 53.70; H, 5.06; N, 16.34. Found: C, 53.79; H, 4.98; N, 16.29.

(h) *Ethyl-6-amino-5-cyano-2-methyl-4-((1R,2S,3S,4S)-1,2,3,4-tetrahydroxy-5-(thiazol-2-ylamino)pentyl)nicotinate 9*.

Pale brown crystals from butanol (m.p. 222–224 °C). IR (cm^{-1}) ν : 3381 (OH), 3324, 3225 (NH_2), 3102 (NH), 2220 (CN), 1721 (C=O), 1648, 1600 (C=N). ^1H -NMR (300 MHz, DMSO-d_6) δ (ppm): 1.20 (t, 3H, $\text{CH}_3\text{CH}_2\text{O}$, $J=6$ Hz), 2.50 (s, 3H, CH_3 -pyridine), 2.58 (s, 1H, CHNH -Ar), 3.18–3.40 (broad, 4H, CH_2 & 2CH -glucose), 4.07 (q, 2H, $\text{CH}_3\text{CH}_2\text{O}$, $J=6.6$ Hz), 4.72 (d, 1H, CH -glucose, $J=3.4$ Hz), 5.72–5.94 (m, 4H, 4OH, D_2O Exchangeable), 6.92–7.21 (m, 2H, Ar-H), 8.12 (s, 1H, NH, D_2O Exchangeable), 8.50 (s, 2H, NH_2 , D_2O Exchangeable). MS (m/z): 437 (M^+ , 35.53%). Anal. Calcd for $\text{C}_{18}\text{H}_{23}\text{N}_5\text{O}_6\text{S}$ (437): C, 49.43; H, 5.26; N, 16.02; S, 7.32. Found: C, 49.360; H, 5.30; N, 15.91; S, 7.41.

(i) *Ethyl-6-amino-5-cyano-2-methyl-4-((1R,2S,3S,4S)-1,2,3,4-tetrahydroxy-5-((4-(N-(thiazol-2-yl)sulfamoyl)phenyl)amino)pentyl)nicotinate (10)*.

Off white crystals from acetone (m.p. 178–180 °C). IR (cm^{-1}) ν : 3384, 3324 (OH), 3322, 3225 (NH_2), 3263 3090 (NH), 2219 (CN), 1721 (C=O), 1648 (C=N). ^1H -NMR (300 MHz, DMSO-d_6) δ (ppm): 1.20 (t, 3H, $\text{CH}_3\text{CH}_2\text{O}$, $J=6$ Hz), 2.54 (s, 3H, CH_3 -pyridine), 2.63 (s, 1H, CHNH -Ar), 3.22–3.48 (broad, 4H, CH_2 & 2CH -glucose), 4.07 (q, 2H, $\text{CH}_3\text{CH}_2\text{O}$, $J=6.5$ Hz), 4.76 (d, 1H, CH -glucose, $J=3.4$ Hz), 5.73–5.94 (m, 4H, 4OH, D_2O Exchangeable), 5.77 (s, 1H, NH, D_2O Exchangeable), 6.55–7.46 (m, 6H, Ar-H), 8.48 (s, 2H, NH_2 , D_2O Exchangeable), 12.39 (s, 1H, NH, D_2O Exchangeable). MS (m/z): 592 (M^+ , 4%). Anal. Calcd for $\text{C}_{24}\text{H}_{28}\text{N}_6\text{O}_8\text{S}_2$ (592): C, 48.65; H, 4.73; N, 14.19; S, 10.81. Found: 48.59; H, 4.82; N, 14.21; S, 10.77.

(j) *Ethyl-6-amino-5-cyano-2-methyl-4-((1R,2S,3S,4S)-1,2,3,4-tetrahydroxy-5-((4-(N-(pyrimidin-2-yl)sulfamoyl)phenyl)amino)pentyl)nicotinate (11)*.

White crystals from acetone (m.p. 220–222 °C). IR (cm^{-1}) ν : 3423, 3361, 3354 (OH), 3322, 3225 (NH_2), 3102, 3074 (NH), 2218 (CN), 1720 (C=O), 1649 (C=N). ^1H -NMR (300 MHz, DMSO-d_6) δ (ppm): 1.19 (t, 3H, $\text{CH}_3\text{CH}_2\text{O}$, $J=6$ Hz), 2.50 (s, 3H, CH_3 -pyridine), 2.59 (s, 1H, CHNH -Ar), 3.22–3.36 (broad, 4H, CH_2 & 2CH -glucose), 4.07 (q, 2H, $\text{CH}_3\text{CH}_2\text{O}$, $J=6.6$ Hz), 4.76 (d, 1H, CH -glucose, $J=3.2$ Hz), 5.74–5.93 (m, 4H, 4OH, D_2O Exchangeable), 5.96 (s, 1H, NH, D_2O Exchangeable), 6.57–8.48 (m, 9H, Ar-H & NH_2 , D_2O Exchangeable), 11.23 (s, 1H, NH, D_2O Exchangeable). ^{13}C -NMR (300 MHz, DMSO-d_6) δ (ppm): 14.2, 21.6, 59.5, 60.8, 79.6, 109.5, 111.0, 111.2, 112.2, 115.0, 115.6, 124.9, 129.9, 144.9, 19.1, 153.1, 157.3, 158.3, 165.6, and 168.5. MS (m/z): 587 (M^+ , 2.7%). Anal. Calcd for $\text{C}_{25}\text{H}_{29}\text{N}_7\text{O}_8\text{S}$ (587): C, 51.11 H, 4.94; N, 16.70; S, 5.45. Found: C, 51.04 H, 5.06; N, 16.61; S, 5.47.

(k) *Ethyl-6-amino-5-cyano-4-((1R,2S,3S,4S)-5-((1,5-dimethyl-3-oxo-2-phenyl-2,3-dihydro-1H-pyrazol-4-yl)amino)-1,2,3,4-tetrahydroxypentyl)-2-methylnicotinate (12)*.

Orange crystals from dioxane (m.p. 176–178 °C). IR (cm^{-1}) ν : 3400 (OH), 3334, 3200 (NH_2), 3090 (NH), 2222 (CN), 1721, 1671 (C=O), 1648, 1620 (C=N). ^1H -NMR (300 MHz, DMSO-d_6) δ (ppm): 1.19 (t, 3H, $\text{CH}_3\text{CH}_2\text{O}$, $J=6$ Hz), 2.23 (s, 3H, CH_3 -C=C), 2.51 (s, 3H, CH_3 -pyridine), 2.57 (s, 1H, CHNH -Ar), 3.24–3.45 (broad, 7H, CH_2 , 2CH -glucose & CH_3 -N), 4.07 (q, 2H, $\text{CH}_3\text{CH}_2\text{O}$, $J=6.5$ Hz), 4.88 (d, 1H, CH -glucose, $J=3.2$ Hz), 5.72–5.95 (m, 4H, 4OH, D_2O Exchangeable), 7.00–7.47 (m, 5H, Ar-H), 8.50 (s, 2H, NH_2 , D_2O Exchangeable), 10.86 (broad, 1H, NH, D_2O Exchangeable). ^{13}C -NMR (300 MHz, DMSO-d_6) δ (ppm): 12.6, 14.1, 21.4, 35.9, 59.4, 59.9, 60.3, 60.5, 60.7, 79.6, 109.4, 116.3, 117.2, 118.7, 128.3, 133.4, 140.0, 144.1, 146.2, 148.9, 154.6, 155.2, 160.4, 163.3, 167.9, and 170.7. MS (m/z): 540 (M^+ , 17.81%). Anal. Calcd for $\text{C}_{26}\text{H}_{32}\text{N}_6\text{O}_7$ (540): C, 57.78 H, 5.93; N, 15.56. Found: C, 57.60 H, 6.01; N, 15.51.

Comparison between microwave and thermal methods

In the microwave reactions, the amount of the same reactants in the thermal technique was used. The reaction completion was illustrated by using TLC. The reaction mixtures were washed with ethanol and crystallized from a suitable solvent. The thermal and microwave reaction times are shown in (Table 1). Comparisons in terms of yields and times between the prepared compounds by using thermal and microwave techniques were reported. However, we used the yield economy (YE) as a term to determine the thermal and microwave synthetic different efficiencies of the same reaction. Calculation of YE was occurred through: $\text{YE} = \frac{\text{yield}\%}{\text{Reaction time}^{\text{min}}}$. In this report, the YE was used to provide the yields obtained conclusively enhanced under microwave and thermal conditions. The equation of RME is: $\text{RME} = \frac{\text{Wt of isolated product}}{\text{Wt of reactants}}$. While, OE was used for the direct comparisons between the two reaction types and can be calculated through $\text{OE} = \frac{\text{RME}}{\text{AE}} \times 100$. So, we can consider the yield economy (YE) as a metric to enhance the conversion efficiencies of these two different synthetic methods of the same reaction. The reaction's theoretical maximum efficiency was represented by using AE, while RME gives the observed mass efficiency. The thermal and microwave reactions atomic economy (AE) have the same values due to using two different reaction conditions to obtain the same desired compounds, as shown in (Table 1).

Cytotoxicity assay

Three human tumour cell lines namely, Hepatocellular carcinoma (HepG2), Mammary gland breast cancer (MCF-7) and Colorectal adenocarcinoma (Caco-2). The cell lines were obtained from ATCC via Holding company for biological products and vaccines (VACSERA), Cairo, Egypt. Doxorubicin was used as a standard

Cpd. no	Time "min"		Yield %		YE		RME		OE		AE
	Th	M.W	Th	M.W	Th	M.W	Th	M.W	Th	M.W	
1	120	2	52	95	0.4333	47.50	32.39	59.17	46.53	85.00	69.61
2	720	12	55	96	0.0764	8	38.21	66.69	48.52	84.69	78.75
3	600	10	58	90	0.0967	9	41.11	63.79	52.13	80.89	78.86
4	960	11	53	92	0.0552	8.36	37.23	64.62	46.91	81.43	79.36
5	1200	12	58	95	0.0483	7.92	49.63	67.84	61.83	84.51	80.27
6	1440	14	56	94	0.0389	6.71	41.70	69.99	50.48	84.72	82.61
7	1200	11	55	96	0.0458	8.73	40.62	70.90	49.45	86.31	82.15
8	1140	10	57	97	0.0500	9.70	41.68	70.92	51.08	86.92	81.59
9	1080	9	58	89	0.0537	9.89	40.49	62.13	51.24	78.63	79.02
10	960	8	59	93	0.0615	11.63	44.72	70.49	53.48	84.30	83.62
11	600	8	55	94	0.0917	11.75	41.60	71.11	49.82	85.16	83.50
12	360	4	53	96	0.1472	24	39.15	70.92	47.70	86.41	82.07

Table 1. Show the comparison in terms of physical data between the synthesized compounds under thermal and microwave techniques.

anticancer drug for comparison. The reagents RPMI-1640 medium, MTT and DMSO (sigma Co., St. Louis, USA), Fetal Bovine serum (GIBCO, UK).

MTT assay: The cell lines mentioned above were used to determine the inhibitory effects of compounds on cell growth using the MTT assay. This colorimetric assay is based on the conversion of the yellow tetrazolium bromide (MTT) to a purple formazan derivative by mitochondrial succinate dehydrogenase in viable cells. Cell lines were cultured in RPMI-1640 medium with 10% fetal bovine serum. Antibiotics added were 100 units/ml penicillin and 100 µg/ml streptomycin at 37 C in a 5% Co2 incubator. The cell lines were seeded in a 96-well plate at a density of 1.0×10^4 cells/well. at 37 C for 48 h under 5% Co2. After incubation, the cells were treated with different concentrations of compounds and incubated for 24 h. After 24 h of drug treatment, 20 µl of MTT solution at 5 mg/ml was added and incubated for 4 h. Dimethyl sulfoxide (DMSO) in volume of 100 µl was added into each well to dissolve the purple formazan formed. The colorimetric assay was measured and recorded at the absorbance of 570 nm using a plate reader (EXL 800, USA). The relative cell viability in percentage was calculated as $(A_{570} \text{ of treated samples} / A_{570} \text{ of untreated sample}) \times 100$ (Table 2).

It was noted that compounds 4 and 8 have stronger cytotoxic activities than other compounds with values of 11.7 and 18.53, respectively, because they have hydrophilic and lipophilic parts that compound 4 has a hydroxyl group which increased the solubility of the compound due to ionic group and compound 8 have amine group which is lipophilic and hydrophilic which can interact with water through hydrogen bond.

Structure activity relationship

In the current report, a series of (b) Ethyl-6-amino-5-cyano-2-methyl-4-((1R,2S,3S,4S)-1,2,3,4-tetrahydroxy-5-((Aryl)amino)pentyl) nicotinate derivatives were prepared and tested their cytotoxicity on three cancer cell lines Caco2, HepG2 and MCF-7. Various derivatives were utilized on the position of 5 amino pentyl moiety at Ar

Compound No	In-vitro Cytotoxicity IC50 (µM)*		
	HepG2	Caco-2	MCF-7
DOX	4.50 ± 0.2	12.49 ± 1.1	4.17 ± 0.2
1	27.03 ± 1.9	46.32 ± 2.6	19.17 ± 1.4
2	70.67 ± 3.4	64.05 ± 3.5	53.46 ± 3.1
3	63.48 ± 3.3	83.50 ± 3.9	48.75 ± 2.8
4	11.78 ± 0.9	14.81 ± 1.2	8.76 ± 0.7
5	86.23 ± 4.0	> 100	73.52 ± 3.8
6	55.64 ± 3.1	52.06 ± 2.9	68.75 ± 3.6
7	42.91 ± 2.6	35.96 ± 2.3	38.49 ± 2.4
8	18.53 ± 1.3	23.11 ± 1.8	13.25 ± 1.1
10	36.20 ± 2.4	29.87 ± 2.1	24.82 ± 1.8
11	49.65 ± 2.9	58.42 ± 3.2	41.30 ± 2.6
12	74.95 ± 3.8	92.24 ± 4.6	57.18 ± 3.4

Table 2. Anticancer activity of the synthesized compounds against HepG2, Caco-2 and MCF-7 cell lines. *IC50 (µM): 1–10 (very strong). 11–20 (strong). 21– 50 (moderate). 51–100 (weak) and above 100 (non-cytotoxic). DOX Doxorubicin.

(Fig. 1). First, a 3-hydroxyphenyl substitution $Ar=3-OH-C_6H_4$ forming an 5-((3-hydroxyphenyl)amino)pentyl moiety appeared to give the highest cytotoxic activity. Furthermore, modulations were performed where Ar was a different aromatic and heterocyclic groups which showed a strong decrease in activities. While a 1,4-dioxo-1,2,3,4-tetrahydrophthalazin-5-yl moiety compound 8 caused a moderated cytotoxic activity effect. However, a 4-(N-(thiazol-2-yl)sulfamoyl)phenyl compound 10 showed a continuously dramatic cytotoxic activity decrease. Moreover, modulations of the Aryl substitution using phenyl, 4-methoxyphenyl, 4-(N-(diaminomethylene)sulfamoyl)phenyl, 4-((E)-phenyldiazenyl)phenyl, 4-(N-(pyrimidin-2-yl)sulfamoyl) phenyl and 1,5-dimethyl-3-oxo-2-phenyl-2,3-dihydro-1H-pyrazol-4-yl caused further cytotoxic activity decreasing. Finally, using 4-acetylphenyl as elucidated in compound 5 displayed the lowest cytotoxic activity through the studied series.

Radiosynthesis and in-vivo biodistribution of radioiodinated compound 4

Synthesis of radioiodinated compound 4

Radioactive iodine (I-131) was electrophilically introduced in compound 4 by using chloramine-T which oxidize $[^{131}I]iodide$ to $[^{131}I]iodonium$ form^{49,50}. The radiolabeling process was carried out through the optimization of different parameters: Chloramine-T: from 100 to 600 μg , pH: from 4 to 9, Compound 4 content: from 100 to 600 μg , and Reaction time: from 15 min to 24 h. Radioiodinated compound 4 formation was calculated by chromatographic technique using paper chromatography and TLC to evaluate the highest radiochemical purity.

In-vivo studies of the radioiodinated compound 4 in sarcoma-bearing mice

Ethical statement

All animal procedures and experimental protocols were performed following the International Guiding Principles for Biomedical Research Involving Animals⁵¹ and were approved by the research ethics committee, Ain Sams University, Egypt (code: ASU-SCI/CHEM/2023/4/1). The current study adheres to the ARRIVE guidelines for reporting in-vivo experiments⁵².

Sarcoma was induced in mice model using the Ehrlich cell line in the right thigh muscle by intramuscularly injecting 100 μL of the cell line suspension (12.5×10^6 cells ml^{-1})⁵³. Female Swiss albino mice were collected in five groups (20–25 g). About 50 μL radioiodinated-compound 4 containing about 5 MBq were intravenously injected. After the pre-determined time, mice were anesthetized using isoflurane, then they were dissected. The body organs of interest and fluids were collected and weighed. The radioactivity of each organ was counted using a NaI (Tl) crystal gamma counter. Bone, blood, and muscles were evaluated as 10, 7, and 40% of the body weight, respectively⁵⁴. % Injected dose per gram (% ID/gram \pm S.D.) was calculated at each time point for each group.

Results and discussion

Synthesis

The ethyl-6-amino-5-cyano-2-methyl-4-((1S,2R,3R,4R)-1,2,3,4,5-pentahydroxypentyl) nicotinate (1) was synthesized through condensation of D-glucose, malonitrile, ethyl acetoacetate and ammonium acetate in ethanol via a new one-pot four component methodology (Scheme 1). The structure of compound 1 was illustrated using mass spectrum which showed a molecular ion peak at $m/z=355$ (M^+ , 31.30%) corresponding to molecular formula $C_{15}H_{21}N_3O_7$.

Compound 1 probably formed through the supposed mechanism shown in (Scheme 2). Compound 1 may occur firstly through a nucleophilic attack from ammonium acetate on malonitrile with the removal of one acidic hydrogen-formed carbanion, which attacks the C=O of the D-glucose followed by removing one molecule of water to give Schiff base. Secondary nucleophilic attack from ammonium acetate on ethyl acetoacetate with the removal of one acidic hydrogen formed carbanion, which makes 1,4-addition with the Schiff base followed by cyclization formed 1,4-dihydropyridine. Finally, occur aromatization by autoxidation at room temperature. Also, Compound 1 probably formed through the supposed mechanism shown in (Scheme 2). Proton transfer from the N-atom on the 1,4-dihydropyridine ring initiates the aromatization of Hantzsch dihydropyridines by

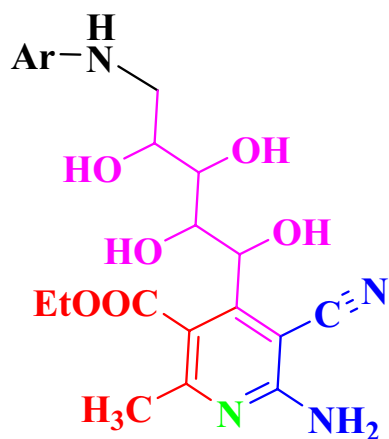
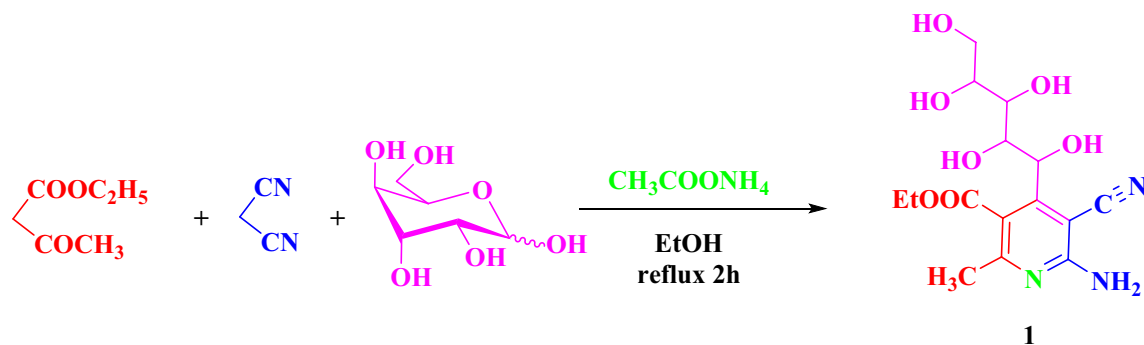


Figure 1. Main nucleus for the synthesized derivatives.



Scheme 1. Formation of ethyl 16-amino-5-cyano-2-methyl-4-(1,2,3,4,5-pentahydroxypentyl) nicotinate, **1**.

superoxide. This anion dihydropyridine then easily passes through additional homogenous oxidations to provide the final aromatized products^{55–57}.

Reactions of compound **1** toward nitrogen nucleophiles such as aromatic and heterocyclic amines namely aniline, 4-methoxy aniline, 3-aminophenol, 4-aminoacetophenone, sulphaguanidine, 4-aminoazobenzene, 5-amino-2,3-dihydrophthalazine-1,4-dione, 2-aminothiazole, 4-amino-N-(thiazol-2-yl)benzenesulfonamide, 4-amino-N-(pyrimidin-2-yl)benzenesulfonamide, 4-aminoantipyrine have been investigated and produced the corresponding condensed compounds **2–12**, which were expected to have some interesting biological activities (Scheme 3).

Compounds **2–12** probably formed through the supposed mechanism shown in (Scheme 4).

Cytopathological examinations

Cultured breast cancer (MCF-7), colon cancer (Caco-2) and hepatocellular carcinoma (HepG2). The cell lines were obtained from ATCC via Holding company for biological products and vaccines (VACSERA), Cairo, Egypt, cells were trypsinized, washed in PBS, pH=7.4 and collected in a tube. The samples were centrifuged at a rate of 1200–1500 r/min for 15 min using Shandon Cytospin (Thermo Fisher Scientific, Waltham, Massachusetts). The cell pellet was spread on glass slides. Slides were immediately fixed in 95% ethanol for 24 h. The slides were stained with hematoxylin and eosin (H & E).

It was noted from Figs. 2, 3 and 4 that cells treated with compounds 4 and 8 showed a moderate number of cancer cells with central nuclei (black arrow) and with scattered apoptotic and degenerative changes compared with control (untreated cell) which have high nucleocytoplasmic ratio and showing a large number of neoplastic cancer cell consisting of groups of epithelial cells with enlarged nuclei.

Radiosynthesis and in-vivo studies of radioiodinated compound 4

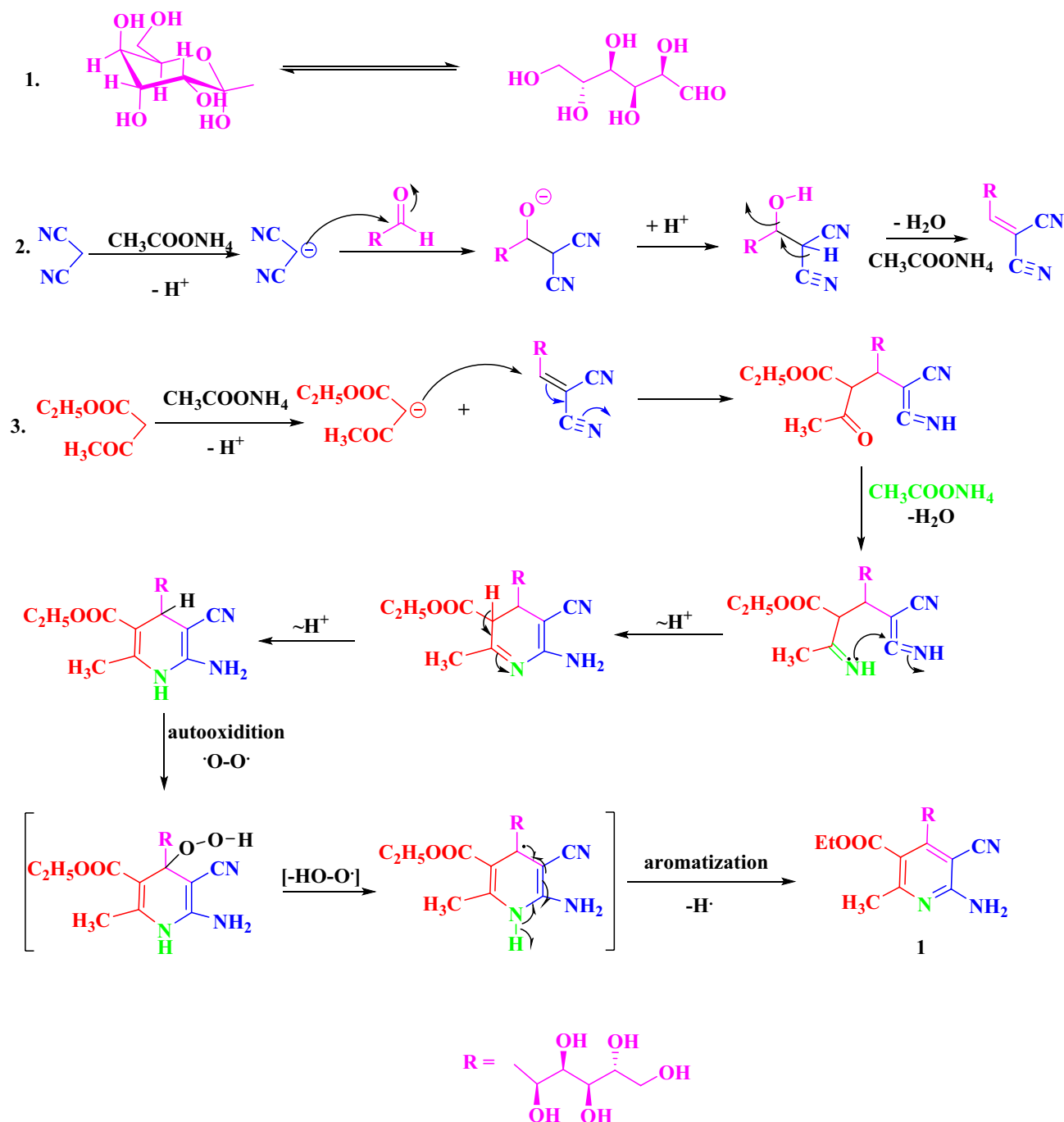
The ADME parameters of the synthesized compounds were intensively studied using the field of radiopharmaceutical chemistry⁵³. Due to radioiodine's high compatibility with a variety of organic compounds and simple physical radio-imaging screening, radioiodine is particularly successful at radioiodinating organic compounds to act as a screening probe of their in-vivo biodistribution pattern⁵³. Considering that among all the investigated compounds, compound 4 showed the highest cytotoxicity. So, it was chosen for investigations on radiolabeling and biodistribution.

Radiosynthesis of radioiodinated compound 4

Compound 4 was radiolabeled with iodine-131 to assess its pharmacokinetics and to study its ability to deliver the therapeutic radioisotope (iodine-131) to the target site (cancer) for radioisotope-targeted therapy. The highest radiochemical purity of radioiodinated compound 4 was achieved via the optimization of all variables. Iodine-131 was electrophilically substituted while being exposed to an oxidizing agent (chloramine-T). The radioiodination process is significantly impacted by chloramine-T, which transforms iodide ions into iodonium ions and also allows an electrophilic substitution to take place⁵⁸. Figure 5 demonstrates that the best dose of 400 µg of CAT results in the highest RCP of 95.59%. Low or high levels of CAT may be the cause of insufficient oxidation of I-131 and unwanted oxidative byproduct⁵⁹. The pH levels of the reaction mixture had a big impact on RCP. The RCP was increased by raising pH from acidic to almost neutral levels (pH 8) and decreased by lowering pH levels by more than 8 (Fig. 6). This drop in RCP may be caused by the creation of iodate (IO₃⁻) and hypoiodite (IO⁻) ions⁶⁰. Figure 7 illustrates the influence of compound 4 (substrate) amount on the RCP. The maximum RCP was obtained at 100 µg of substrate, which may capture every iodonium ion from the reaction mixture. There are no appreciable variations in RCP as substrate amounts are increased. Figure 8 depicts the speed of this reaction and the stability of the radioiodinated molecule that resulted. After 30 min, the reaction was finished, and a 24-h stability study was conducted. (supplementary file).

In-vivo studies of radioiodinated compound 4 in a sarcoma-bearing mice

Biodistribution of radioiodinated compound 4 in the animal modes indicates that most organs have no specific accumulation in all non-target organs and showed rapid clearance from soft tissues (Fig. 9A). The targeting

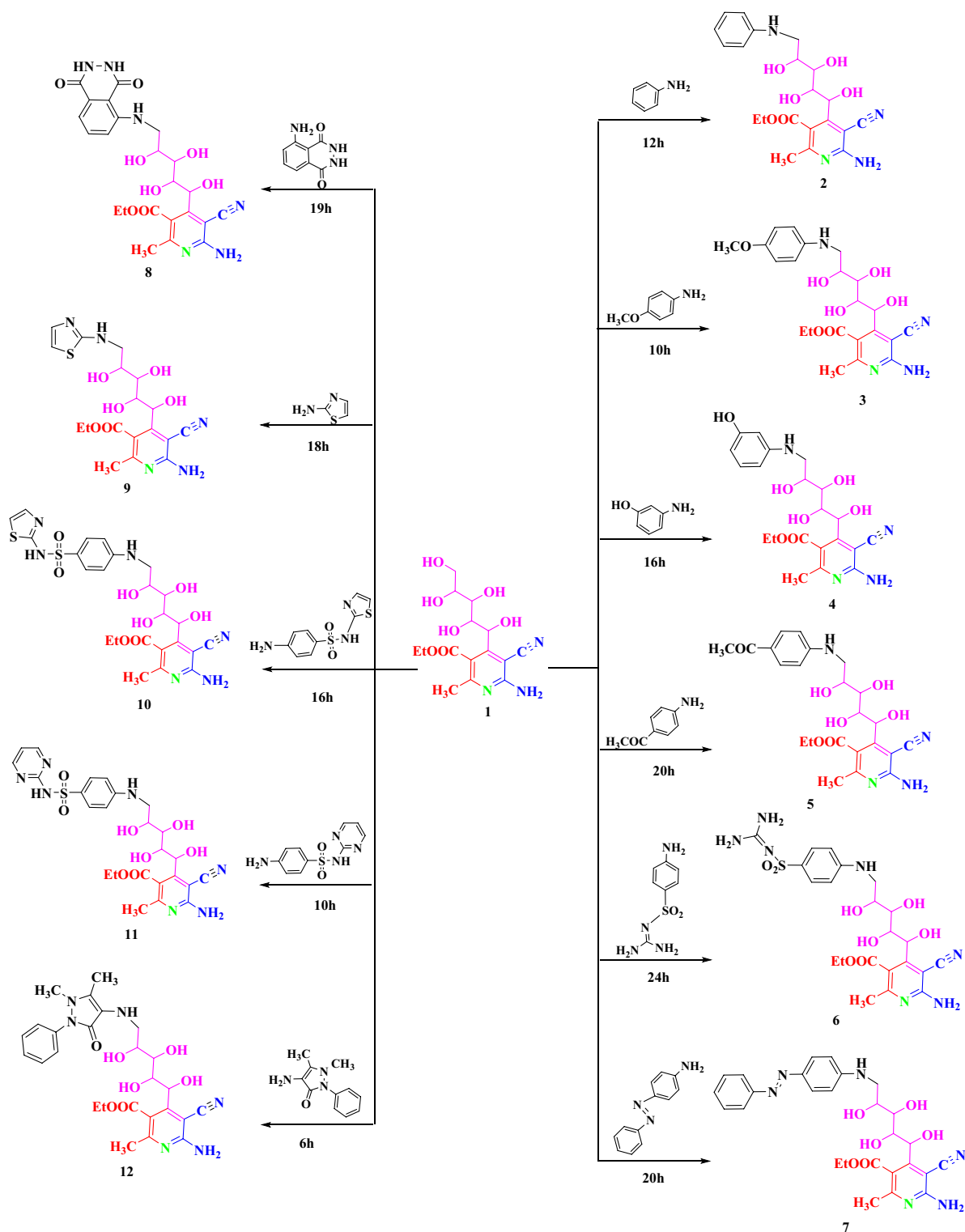


Scheme 2. Mechanism of formation of pyridine derivative, 1.

ability of radioiodinated compound **4** towards cancer cells was studied in murine-bearing sarcoma. Figure 9B illustrates the tumor uptake showing higher values in all studied time points in a comparison with normal sites. Furthermore, T/NT (target to non-target ratio) was greater than one-fold at all time points, reaching its highest value at one hour post-injection with a value of 3.86 (Fig. 9C). This high ratio (T/NT) indicates that radioiodinated compound **4** can target cancer sites efficiently. The radioiodinated compound **4** was excreted through both urinary and hepatobiliary pathways, this was cleared in Fig. 9D which detected accumulation in the organs of excretion (kidneys and liver). (supplementary file).

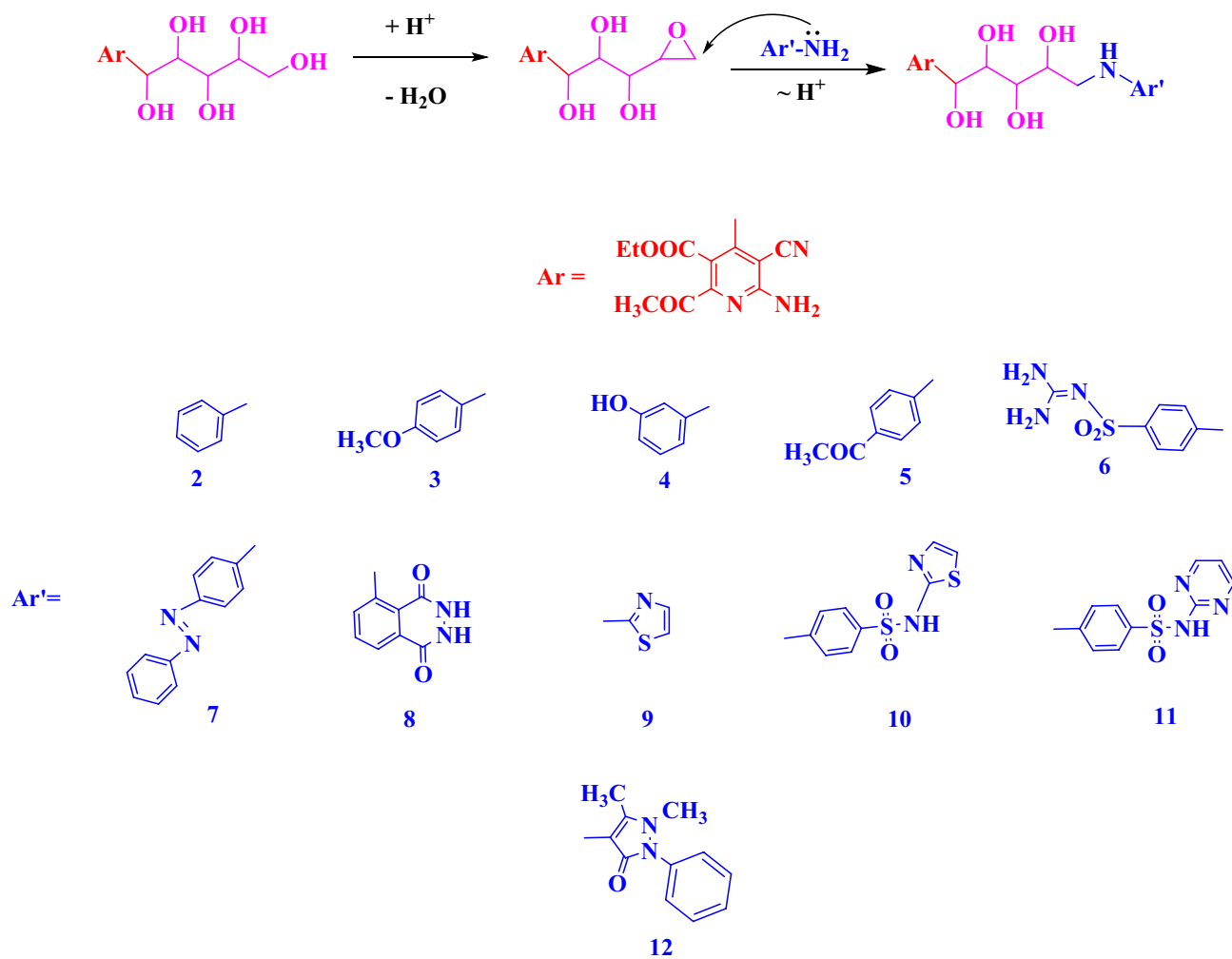
Conclusion

Our strategy for the synthesis of ethyl-6-amino-5-cyano-2-methyl-4-((1S,2R,3R,4R)-1,2,3,4,5-pentahydroxypentyl) nicotinate **1** was simply through a multicomponent reaction of D-glucose, malononitrile and ethyl acetoacetate in the presence of ammonium acetate. Then, the preparation of thirteen molecularly designed nicotinate derivatives was performed from the reactions of



Scheme 3. Formation of compounds 2–12.

ethyl-6-amino-5-cyano-2-methyl-4-((1S,2R,3R,4R)-1,2,3,4,5-pentahydroxypentyl) nicotinate **1** with some selected aromatic and heterocyclic amines. All the newly synthesized compounds were prepared by conventional method and under microwave irradiation. The anti-cancer and biological activities of the produced compounds have been evaluated. Also, it was noted that compounds **4** and **8** have stronger cytotoxic activities than other compounds because they have hydrophilic and lipophilic parts. The radioiodinated compound **4** can target the cancer site efficiently. After careful studies, the newly synthesized compounds may be promising candidates as novel cancer theranostic agents.



Scheme 4. Mechanism of formation of compounds 2–12.

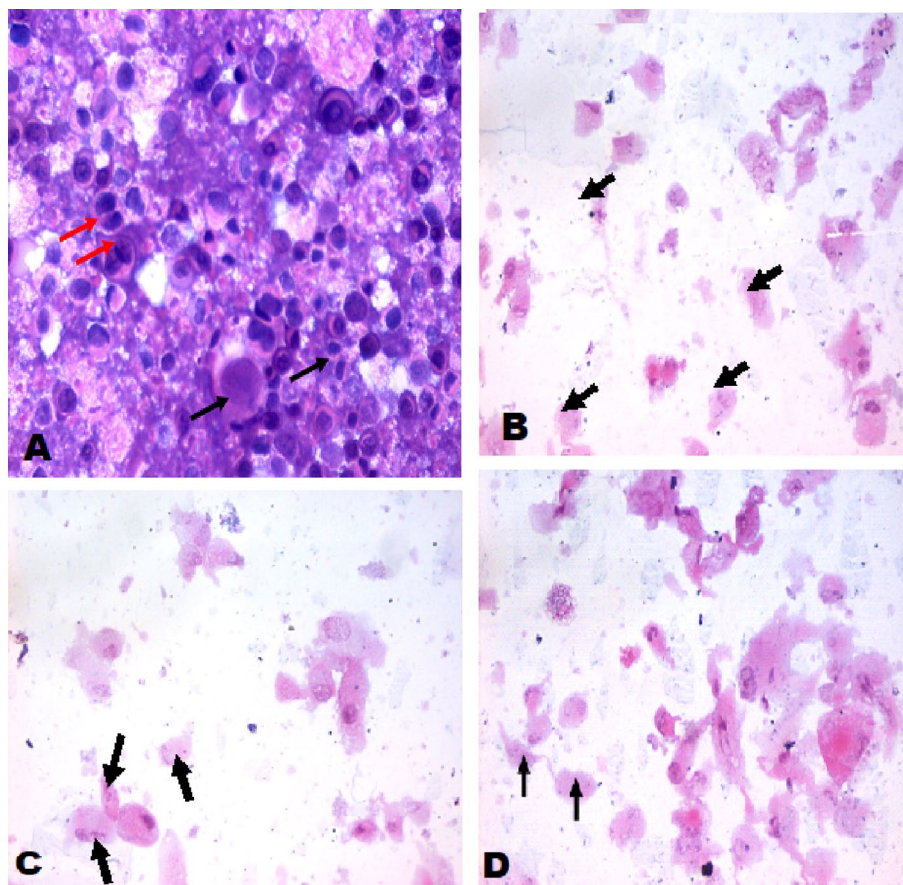


Figure 2. Cytospin smear stained by H & E (400×). (A) Untreated colon carcinoma cell line (Caco-2) cell, (B) (Caco-2) cells treated with the Doxorubicin was used as a standard anticancer drug, (C) Caco-2) cells treated with the compound 4, (D) Caco-2) cells treated with the compound 8.

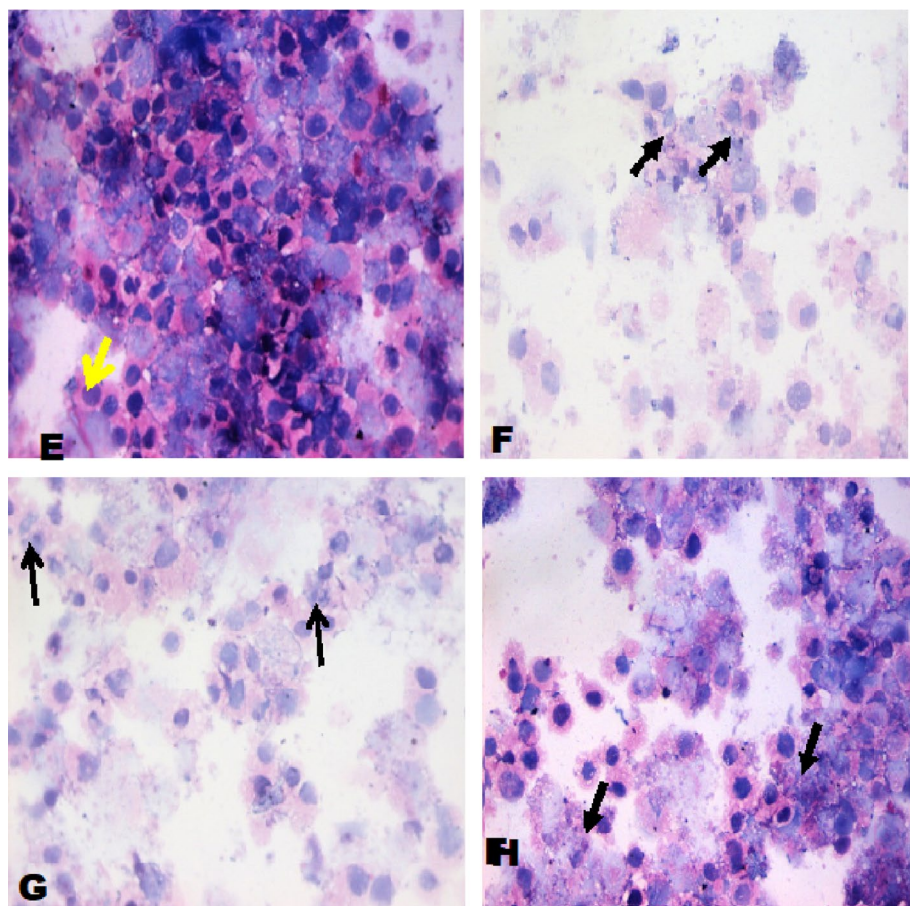


Figure 3. Cytospin smear stained by H & E (400×). E- Untreated hepatocellular carcinoma (HepG2) cells F- HepG2 cells treated with the Doxorubicin was used as a standard anticancer drug, G- HepG2 cells treated with the compound 4, H: HepG2 cells treated with the compound 8.

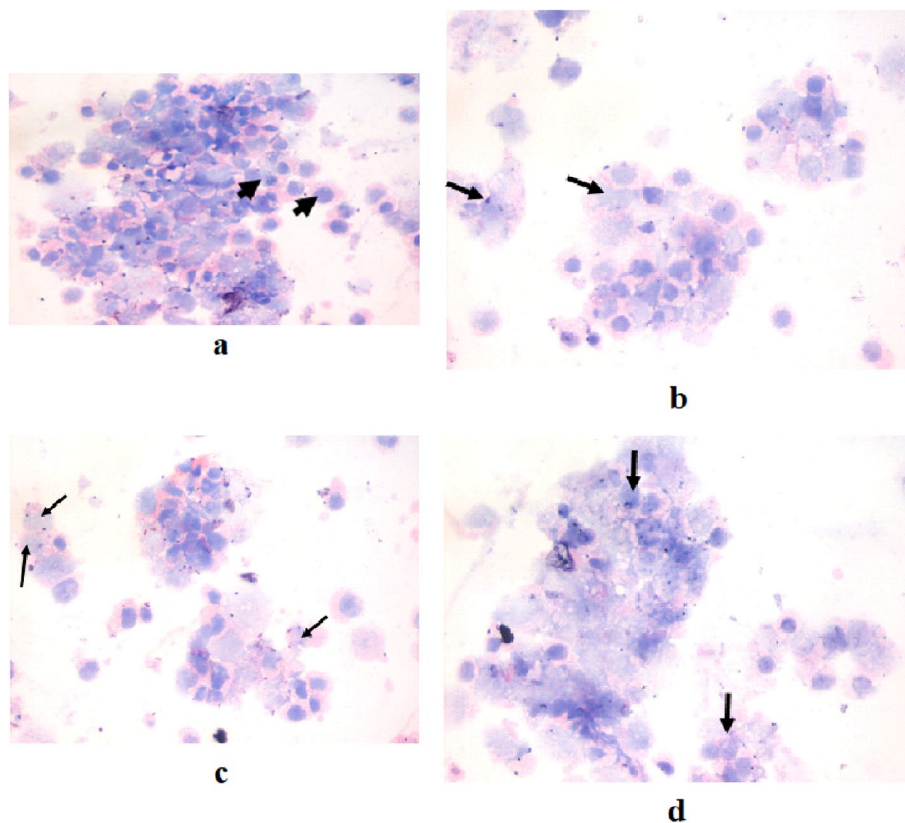


Figure 4. Cytospin smear stained by H & E (400×). A- Untreated Mammary gland breast cancer (MCF-7) cells, b- Mammary gland breast cancer (MCF-7) treated with the Doxorubicin was used as a standard anticancer drug, c- Mammary gland breast cancer (MCF-7) cells treated with the compound 4, d- Mammary gland breast cancer (MCF-7) treated with the compound 8.

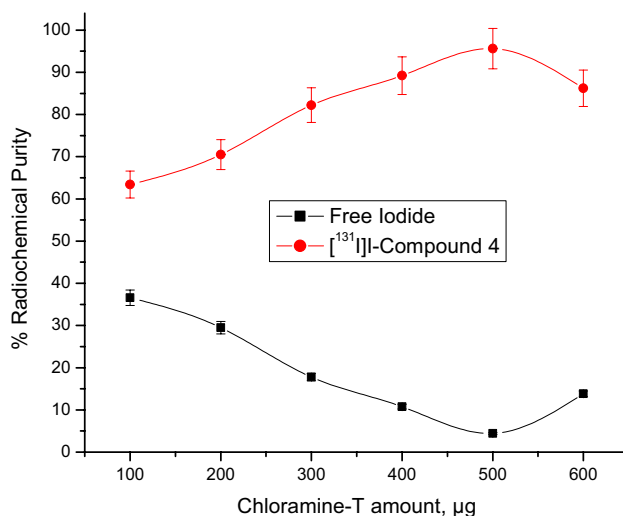


Figure 5. Impact of CAT amount on RCP of [¹³¹I]-compound 4. Conditions for the reaction: 400 µg of compound 4, pH 8, and 5 µl of [¹³¹I] NaI solution (3.7 MBq) after 30 min at room temperature, N=5 separate tests.

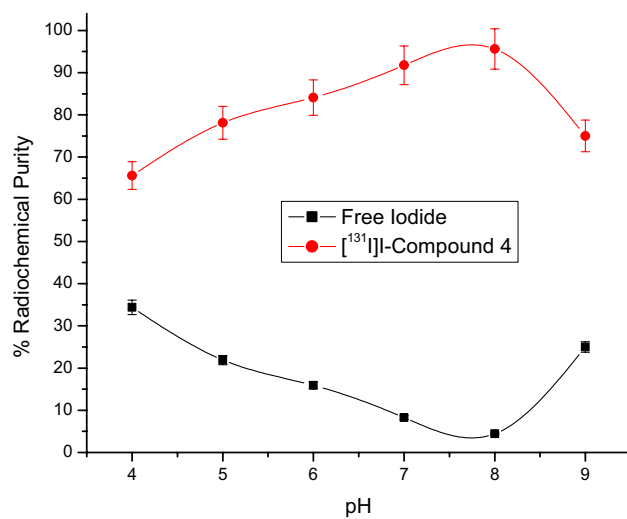


Figure 6. Impact of pH on RCP of ^{131}I -compound 4. Conditions for the reaction: 500 μg of CAT, 400 μg of compound 4, and 5 μl of ^{131}I NaI solution (3.7 MBq) after 30 min at room temperature, N=5 separate tests.

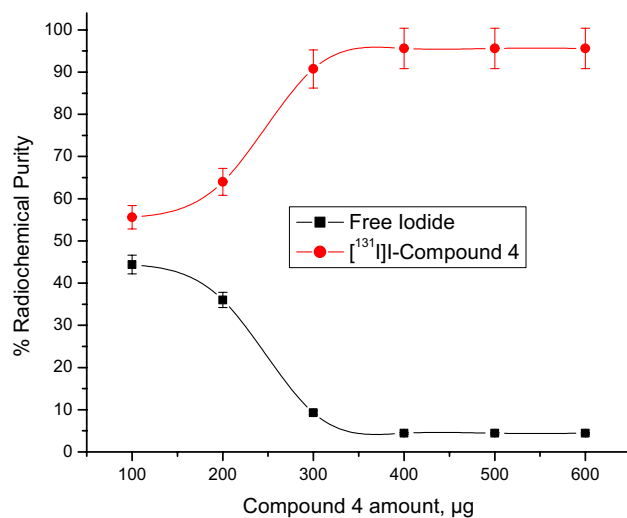


Figure 7. Impact of compound 4 amount on RCP of ^{131}I -compound 4. Conditions for the reaction: 500 μg of CAT, pH 8 and 5 μl of ^{131}I NaI solution (3.7 MBq) after 30 min at room temperature, N=5 separate tests.

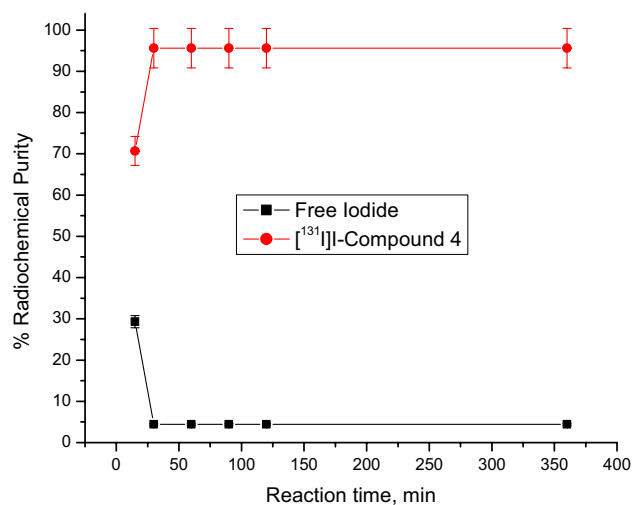


Figure 8. Impact of reaction time on RCP of [¹³¹I]I-compound 4. Conditions for the reaction: 500 µg of CAT, 400 µg of compound 4, pH 8 and 5 µl of [¹³¹I] NaI solution (3.7 MBq) at room temperature, N=5 separate tests.

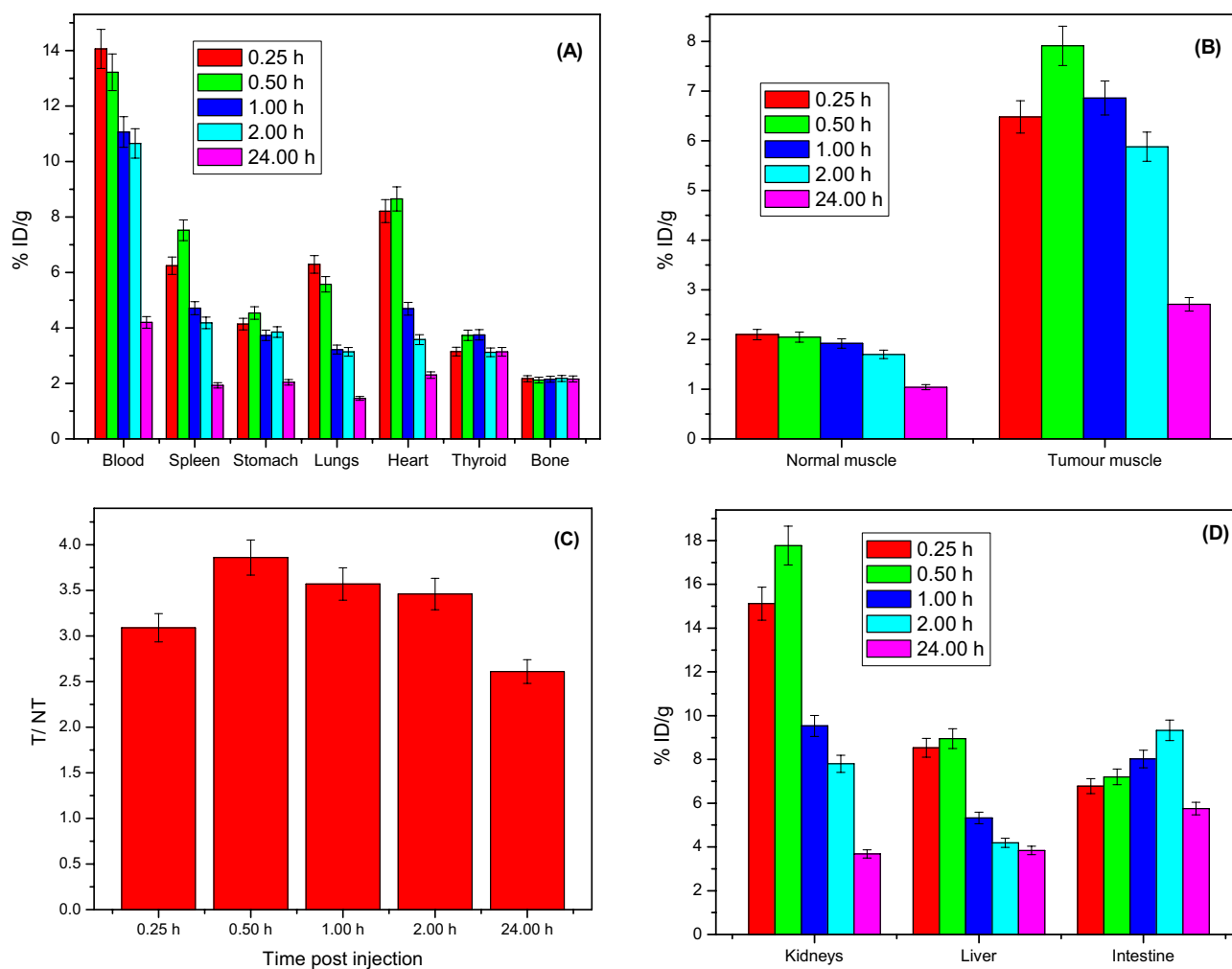


Figure 9. % ID/g organ of the radioiodinated compound 4 in tumour bearing mice (A) non-target organs (B) % ID/g organ in normal and tumour muscles (C) tumour muscles/normal muscles (T/NT) (D) excretory organs.

Data availability

All data generated or analyzed during this study are included in this published article.

Received: 15 May 2023; Accepted: 30 January 2024

Published online: 01 February 2024

References

- Das, C., Kastania, E., Witt, J. & Ozcan, O. Corrosion protection properties of poly (4-vinyl pyridine) containing multilayer polymeric coatings on magnesium alloy AZ31. *Mater. Corros.* **73**, 427–435 (2022).
- Rezaeivala, M., Karimi, S., Tuzun, B. & Sayin, K. Anti-corrosion behavior of 2-((3-(2-morpholino ethylamino)-N3-((pyridine-2-yl) methyl) propylimino) methyl) pyridine and its reduced form on Carbon Steel in Hydrochloric Acid solution: Experimental and theoretical studies. *Thin Solid Films* **741**, 139036 (2022).
- Tseberlidis, G., Intrieri, D. & Caselli, A. Catalytic applications of pyridine-containing macrocyclic complexes. *Eur. J. Inorg. Chem.* **2017**, 3589–3603 (2017).
- Kang, N.-G., Kang, B.-G., Koh, H.-D., Changez, M. & Lee, J.-S. Block copolymers containing pyridine moieties: Precise synthesis and applications. *React. Funct. Polym.* **69**, 470–479 (2009).
- Mohamed, E. A., Ismail, N. S., Hagrass, M. & Refaat, H. Medicinal attributes of pyridine scaffold as anticancer targeting agents. *Future J. Pharm. Sci.* **7**, 1–17 (2021).
- Badger, M. R., Palmqvist, K. & Yu, J. W. Measurement of CO₂ and HCO₃⁻ Fluxes in cyanobacteria and microalgae during steady-state photosynthesis. *Physiol. Plant.* **90**, 529–536 (1994).
- Pastorekova, S. & Gillies, R. J. The role of carbonic anhydrase IX in cancer development: Links to hypoxia, acidosis, and beyond. *Cancer Metastasis Rev.* **38**, 65–77 (2019).
- Liu, S. *et al.* Design, synthesis and biological evaluations of 2-amino-4-(1-piperidine) pyridine derivatives as novel anti crizotinib-resistant ALK/ROS1 dual inhibitors. *Eur. J. Med. Chem.* **179**, 358–375 (2019).
- Sangani, C. B. *et al.* Design, synthesis and molecular modeling of biquinoline—Pyridine hybrids as a new class of potential EGFR and HER-2 kinase inhibitors. *Bioorg. Med. Chem. Lett.* **24**, 4472–4476 (2014).
- Subbaramaiah, V., Srivastava, V. C. & Mall, I. D. Catalytic activity of Cu/SBA-15 for peroxidation of pyridine bearing wastewater at atmospheric condition. *AIChE J.* **59**, 2577–2586 (2013).
- Zalat, O. & Elsayed, M. A study on microwave removal of pyridine from wastewater. *J. Environ. Chem. Eng.* **1**, 137–143 (2013).
- Ali, E. M. *et al.* Design, synthesis and anti-inflammatory activity of imidazol-5-yl pyridine derivatives as p38α/MAPK14 inhibitor. *Bioorg. Med. Chem.* **31**, 115969 (2021).
- El-Sharkawy, K. A., AlBratty, M. M. & Alhazmi, H. A. Synthesis of some novel pyrimidine, thiophene, coumarin, pyridine and pyrrole derivatives and their biological evaluation as analgesic, antipyretic and anti-inflammatory agents. *Braz. J. Pharm. Sci.* **54**, e00153 (2019).
- Ceglowski, M. *et al.* Molecularly imprinted polymers with enhanced selectivity based on 4-(aminomethyl) pyridine-functionalized poly (2-oxazoline)s for detecting hazardous herbicide contaminants. *Chem. Mater.* **34**, 84–96 (2021).
- N'Guessan, J.-P.D.U. *et al.* Discovery of imidazo [1,2-a] pyridine-based anthelmintic targeting cholinergic receptors of *Haemonchus contortus*. *Bioorg. Med. Chem.* **25**, 6695–6706 (2017).
- Satpathi, D. *et al.* Development of DNA intercalative, HSA binder pyridine-based novel Schiff base Cu(II), Ni(II) complexes with effective anticancer property: A combined experimental and theoretical approach. *Appl. Organomet. Chem.* **36**, e6473 (2022).
- Alizadeh, S. R. & Ebrahimzadeh, M. A. Antiviral activities of pyridine fused and pyridine containing heterocycles, a review (from 2000 to 2020). *Mini. Rev. Med. Chem.* **21**, 2584–2611 (2021).
- Althagafi, I. Molecular modeling and antioxidant evaluation of new di-2-thienyl ketones festooned with thiazole or pyridine moiety. *J. Mol. Struct.* **1247**, 131287 (2022).
- Li, P., Yang, Z. & Wang, X. Design, synthesis, and insecticidal activity of novel diacylhydrazine derivatives containing an isoxazole carboxamide or a pyridine carboxamide moiety. *Russ. J. Gen. Chem.* **92**, 132–140 (2022).
- Fayed, E. A., Nosseir, E. S., Atef, A. & El-Kalyoubi, S. A. In vitro antimicrobial evaluation and in silico studies of coumarin derivatives tagged with pyrano-pyridine and pyrano-pyrimidine moieties as DNA gyrase inhibitors. *Mol. Divers.* **26**, 341–363 (2021).
- Abubshait, S. A. *et al.* SPIONs as a nanomagnetic catalyst for the synthesis and anti-microbial activity of 2-aminothiazoles derivatives. *Arab. J. Chem.* **15**, 103878 (2022).
- Anwer, K. E., El-Sattar, N. E. A., Shamaa, M. M., Zakaria, M. Y. & Beshay, B. Y. Design, green synthesis and tailoring of vitamin E TPGS augmented niosomal nano-carrier of pyrazolopyrimidines as potential anti-liver and breast cancer agents with accentuated oral bioavailability. *Pharmaceuticals* **15**, 330 (2022).
- Babamale, H. F., Khor, B. K., Chear, N. J. Y. & Yam, W. S. Safe and selective anticancer agents from tetrafluorinated azobenzene-imidazolium ionic liquids: Synthesis, characterization, and cytotoxic effects. *Archiv der Pharmazie* **355**, 2200085 (2022).
- Gangasani, J. K., Yarasi, S., Naidu, V. G. M. & Vaidya, J. R. Triazine based chemical entities for anticancer activity. *Phys. Sci. Rev.* <https://doi.org/10.1515/psr-2022-0005> (2022).
- Li, W. *et al.* Pyrimidine-fused dinitrogenous penta-heterocycles as a privileged scaffold for anti-cancer drug discovery. *Current Top. Med. Chem.* **22**, 284–304 (2022).
- Xiao-hong, Z., Tong-wei, G., Xu-ran, H., Shi-sheng, W. & Wei-jie, Z. Synthesis and antitumor activity of cyclopamine analogues. *Nat. Product Res. Dev.* **27**, 890 (2015).
- Jin, J., Okagu, O. D. & Udenigwe, C. C. Differential influence of microwave and conventional thermal treatments on digestibility and molecular structure of buckwheat protein isolates. *Food Biophys.* **17**, 198–208 (2022).
- Santos, T., Hennetier, L., Costa, V. & Costa, L. Microwave versus conventional porcelain firing: Colour analysis. *Mater. Chem. Phys.* **275**, 125265 (2022).
- Muškinja, J., Janković, N., Ratković, Z., Bogdanović, G. & Bugarčić, Z. Vanillic aldehydes for the one-pot synthesis of novel 2-oxo-1,2,3,4-tetrahydropyrimidines. *Mol. Divers.* **20**, 591–604 (2016).
- Anwer, K., Sayed, G., Hassan, H. & Azab, M. Conventional and microwave synthesis of some new pyridine derivatives and evaluation their antimicrobial and cytotoxic activities. *Egypt. J. Chem.* **62**, 707–726 (2019).
- Anwer, K. E., Sayed, G. H. & Ramadan, R. M. Synthesis, spectroscopic, DFT calculations, biological activities and molecular docking studies of new isoxazolone, pyrazolone, triazine, triazole and amide derivatives. *J. Mol. Struct.* **1256**, 132513 (2022).
- Sayed, G. H., Azab, M. E. & Anwer, K. E. Conventional and microwave-assisted synthesis and biological activity study of novel heterocycles containing pyran moiety. *J. Heterocycl. Chem.* **56**, 2121–2133 (2019).
- Essa, B. M., Selim, A. A., Sayed, G. H. & Anwer, K. E. Conventional and microwave-assisted synthesis, anticancer evaluation, ^{99m}Tc-coupling and In-vivo study of some novel pyrazolone derivatives. *Bioorg. Chem.* **125**, 105846 (2022).

34. Hussein, E. M., Abulkhair, H. S., El-Dydamony, N. M. & Anwer, K. E. Exploring the cytotoxic effect and CDK-9 inhibition potential of novel sulfaguandinine-based azopyrazolidine-3,5-diones and 3,5-diaminoazopyrazoles. *Bioorg. Chem.* **4**, 106397 (2023).
35. Anwer, K. E., Farag, A. A., Mohamed, E. A., Azmy, E. M. & Sayed, G. H. Corrosion inhibition performance and computational studies of pyridine and pyran derivatives for API X-65 steel in 6 M H₂SO₄. *J. Ind Eng. Chem.* **97**, 523–538 (2021).
36. Farag, A. A., Mohamed, E. A., Sayed, G. H. & Anwer, K. E. Experimental/computational assessments of API steel in 6 M H₂SO₄ medium containing novel pyridine derivatives as corrosion inhibitors. *J. Mol. Liq.* **330**, 115705 (2021).
37. Mohamed, S. S. *et al.* Synthesis and exploring novel annulated 1,3-diphenylpyrazole derivatives as antimicrobial and anticancer agents. *J. Basic Environ. Sci* **8**, 124–139 (2021).
38. Sayed, G. H., Azab, M. E., Anwer, K. E., Raouf, M. A. & Negm, N. A. Pyrazole, pyrazolone and enamionitrile pyrazole derivatives: Synthesis, characterization and potential in corrosion inhibition and antimicrobial applications. *J. Mol. Liq.* **252**, 329–338 (2018).
39. Sayed, G., Negm, N., Azab, M. & Anwer, K. Synthesis, characterization and biological activity of some pyrazole-pyrazolone derivatives. *Egypt. J. Chem.* **59**, 663–672 (2016).
40. Mohamed, S. *et al.* Synthesis and biological activity of a new class of enamionitrile pyrazole. *Egypt. J. Chem.* **64**, 3187–3203 (2021).
41. Anwer, K. E. & Sayed, G. H. Conventional and microwave reactions of 1,3-diaryl-5,4-enamionitrile-pyrazole derivative with expected antimicrobial and anticancer activities. *J. Heterocycl. Chem.* **57**, 2339–2353 (2020).
42. Sayed, G. H., Azab, M. E., Negm, N. A. & Anwer, K. E. Antimicrobial and cytotoxic activities of some novel heterocycles bearing pyrazole moiety. *J. Heterocycl. Chem.* **55**, 1615–1625 (2018).
43. Sadraei, S. L., St Onge, B. & Trant, J. F. Recent advances in the application of carbohydrates as renewable feedstocks for the synthesis of nitrogen-containing compounds. *Phys. Sci. Rev.* **4**, 20180074 (2019).
44. Verma, C. *et al.* Corrosion inhibition of mild steel in 1M HCl by D-glucose derivatives of dihydropyrido[2,3-d:6,5-d']dipyrimidine-2,4,6,8(1H, 3H, 5H, 7H)-tetraone. *Sci. Rep.* **7**, 1–17 (2017).
45. Nourisefat, M., Panahi, F. & Khalafi-Nezhad, A. Carbohydrates as a reagent in multicomponent reactions: One-pot access to a new library of hydrophilic substituted pyrimidine-fused heterocycles. *Org. Biomol. Chem.* **12**, 9419–9426 (2014).
46. Shewaiter, M. A., Selim, A. A., Moustafa, Y. M., Gad, S. & Rashed, H. M. Radioiodinated acemetacin loaded niosomes as a dual anticancer therapy. *Int. J. Pharm.* **628**, 122345 (2022).
47. Essa, B. M., Selim, A. A., El-Kawy, O. & Abdelaziz, G. Preparation and preliminary evaluation study of [131I] iodocolchicine-gallic-AuNPs: A potential scintigraphic agent for inflammation detection. *Int. J. Radiat. Biol.* **98**, 1358–1365 (2022).
48. Selim, A. A., Motaleb, M. & Fayez, H. A. Lung cancer-targeted [131I]-iodoshikonin as theranostic agent: Radiolabeling, in vivo pharmacokinetics and biodistribution. *Pharma. Chem. J.* **55**, 1163–1168 (2022).
49. Taha, E. *et al.* Cod liver oil nano-structured lipid carriers (Cod-NLCs) as a promising platform for nose to brain delivery: Preparation, in vitro optimization, ex vivo cytotoxicity & in vivo biodistribution utilizing radioiodinated zopiclone. *Int. J. Pharm. X* **5**, 100160 (2023).
50. Selim, A. A., Essa, B. M., Abdelmonem, I. M., Amin, M. A. & Sarhan, M. O. Extraction, purification and radioiodination of Khellin as cancer theranostic agent. *Appl. Radiat. Isotop.* **178**, 109970 (2021).
51. Editors-In-Chief. Vol. 8, pp. 265–265 (Taylor & Francis, 1986).
52. McGrath, J. C., Drummond, G., McLachlan, E., Kilkenny, C. & Wainwright, C. Guidelines for reporting experiments involving animals: The ARRIVE guidelines. *Br J Pharmacol* **160**, 1573–1576 (2010).
53. El-Masry, R. M. *et al.* New 5-aryl-1,3,4-thiadiazole-based anticancer agents: Design, synthesis, in vitro biological evaluation and in vivo radioactive tracing studies. *Pharmaceuticals* **15**, 1476 (2022).
54. Fayez, H. & Selim, A. A. Bone targeted new zoledronate derivative: Design, synthesis, 99mTc-coupling, in-silico study and preclinical evaluation for promising osteosarcoma therapy. *Int. J. Radiat. Biol.* **98**, 1664–1672 (2022).
55. Anwer, K. E., Hamza, Z. K. & Ramadan, R. M. Synthesis, spectroscopic, DFT calculations, biological activity, SAR, and molecular docking studies of novel bioactive pyridine derivatives. *Sci. Rep.* **13**, 15598 (2023).
56. Ortiz, M., Núñez-Vergara, L. J., Camargo, C. & Squella, J. Oxidation of Hantzsch 1,4-dihydropyridines of pharmacological significance by electrogenerated superoxide. *Pharm. Res.* **21**, 428–435 (2004).
57. Zhang, D. & Sha, M. Facile aromatisation of Hantzsch 1,4-dihydropyridines by autoxidation in the presence of p-toluenesulfonic acid in acetic acid. *J. Chem. Res.* **42**, 141–144 (2018).
58. Fayez, H., El-Motaleb, M. A. & Selim, A. A. Synergistic cytotoxicity of shikonin-silver nanoparticles as an opportunity for lung cancer. *J. Label. Compd. Radiopharm.* **63**, 25–32 (2020).
59. Abdelaziz, G., Shamsel-Din, H. A., Sarhan, M. O. & Gizawy, M. A. Tau protein targeting via radioiodinated azure A for brain theranostics: radiolabeling, molecular docking, in vitro and in vivo biological evaluation. *J. Label. Compd. Radiopharm.* **63**, 33–42 (2020).
60. Saha, G. B. *Physics and Radiobiology of Nuclear Medicine* (Springer, 2012).

Author contributions

M.M.M. and K.E.A. perform the organic synthesis. A.A.S. performs radioiodination and pharmacokinetic studies. O.A.H., A.A.S., G.H.S. and K.E.A. revise all results. All authors read and approved the final manuscript.

Funding

Open access funding provided by The Science, Technology & Innovation Funding Authority (STDF) in cooperation with The Egyptian Knowledge Bank (EKB).

Competing interests

The authors declare no competing interests.

Additional information

Supplementary Information The online version contains supplementary material available at <https://doi.org/10.1038/s41598-024-53228-4>.

Correspondence and requests for materials should be addressed to A.A.S.

Reprints and permissions information is available at www.nature.com/reprints.

Publisher's note Springer Nature remains neutral with regard to jurisdictional claims in published maps and institutional affiliations.



Open Access This article is licensed under a Creative Commons Attribution 4.0 International License, which permits use, sharing, adaptation, distribution and reproduction in any medium or format, as long as you give appropriate credit to the original author(s) and the source, provide a link to the Creative Commons licence, and indicate if changes were made. The images or other third party material in this article are included in the article's Creative Commons licence, unless indicated otherwise in a credit line to the material. If material is not included in the article's Creative Commons licence and your intended use is not permitted by statutory regulation or exceeds the permitted use, you will need to obtain permission directly from the copyright holder. To view a copy of this licence, visit <http://creativecommons.org/licenses/by/4.0/>.

© The Author(s) 2024